Electronic Supplementary Material (ESI) for Reaction Chemistry & Engineering.

Supporting Information

Effect of Reaction Conditions on the Hydrogenolysis of Polypropylene and Polyethylene into Gas and Liquid Alkanes

Linxiao Chen,§[1] Yifeng Zhu,§[1,2] Laura C. Meyer,[1] Lillian V. Hale,[1] Thuy T. Le,[1] Abhi Karkamkar,[1] Johannes A. Lercher,[1] Oliver Y. Gutierrez,[1]* Janos Szanyi[1]*

[1] Institute for Integrated Catalysis, Pacific Northwest National Laboratory, Richland, WA 99352, USA

[2] Department of Chemistry, Fudan University, 200433, P.R. China

§ These authors contributed equally

Catalyst characterization data

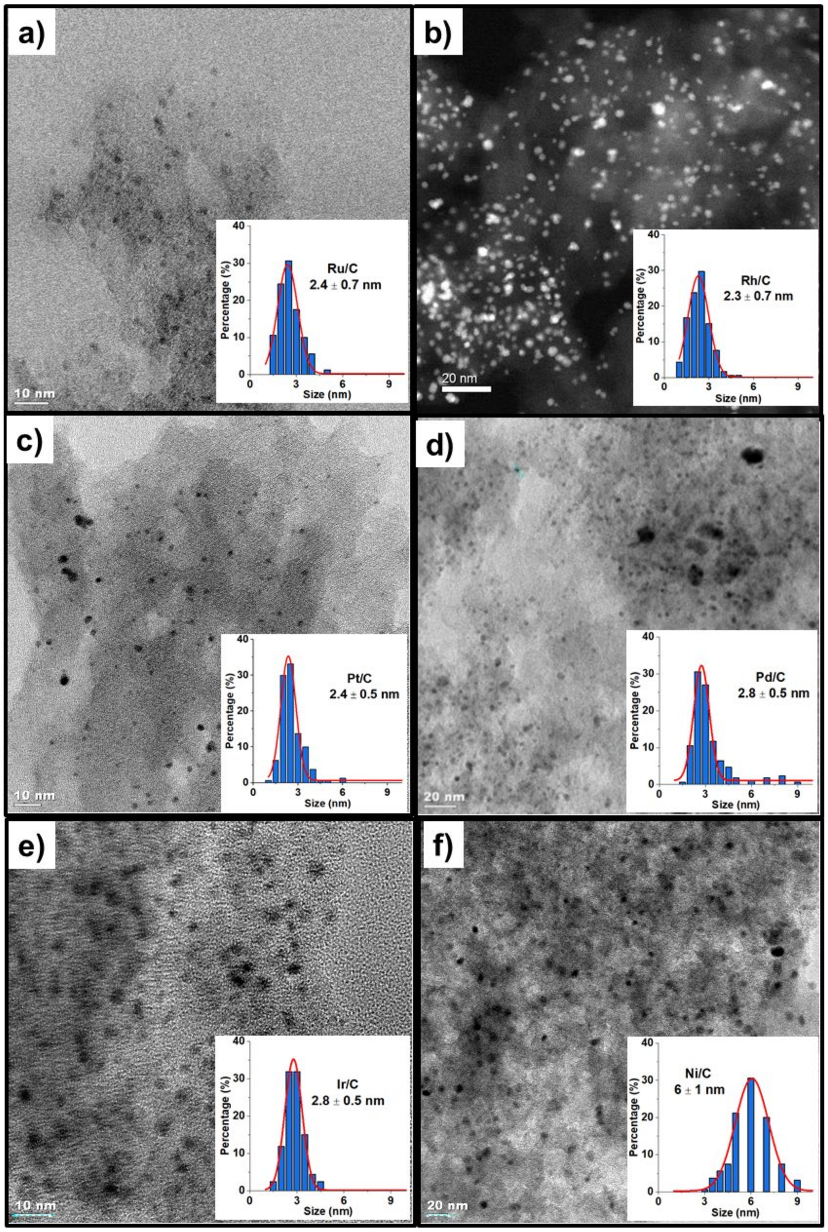

Figure S1. Transmission electron microscopy (TEM) images and particle size distribution of carbon (C)-supported metal catalysts: **a)** ruthenium (Ru)/C; **b)** ruthenium (Rh)/C; **c)** platinum (Pt)/C; **d)** palladium (Pd)/C; **e)** (iridium) (Ir)/C; and **f)** nickel (Ni)/C.

The TEM-derived metal particle size distribution and the average diameter (~2.5 nm standard deviation of ≤0.7 nm) were similar for all catalysts, but Ni/C (~6 ±1 nm, Table 2 and Figure S1).

Table S1. Catalyst characterization results besides TEM

	Ru/C results
Ru loading (inductively coupled plasma mass spectroscopy)	4.16%
Mean Ru size (hydrogen (H_2-chemisorption)	4.7 nm
Ru dispersion (H_2-chemisorption)	23%
BET surface area (nitrogen (N_2)-physisorption)	437 m^2/g
Pore volume (N_2-physisorption)	0.18 cm^3/g
Average pore diameter (N_2-physisorption)	4.8 nm

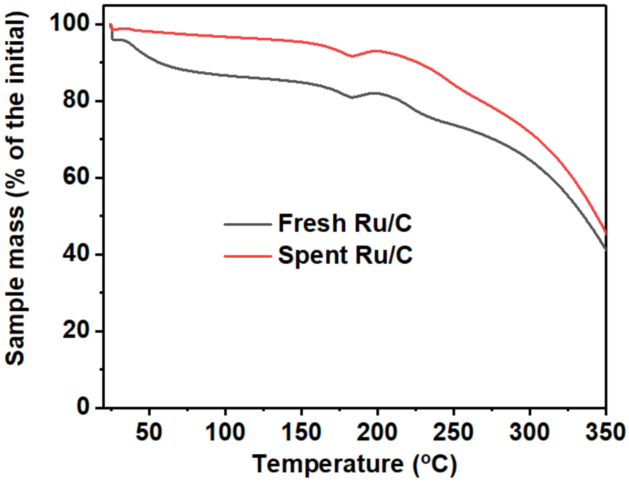

Figure S2. Thermogravimetric analysis (TGA) of Ru/C. Black and red curves show data on the fresh catalyst and the catalyst used in the hydrogenolysis of polyethylene (PE), respectively.

Details on the analysis of liquid products

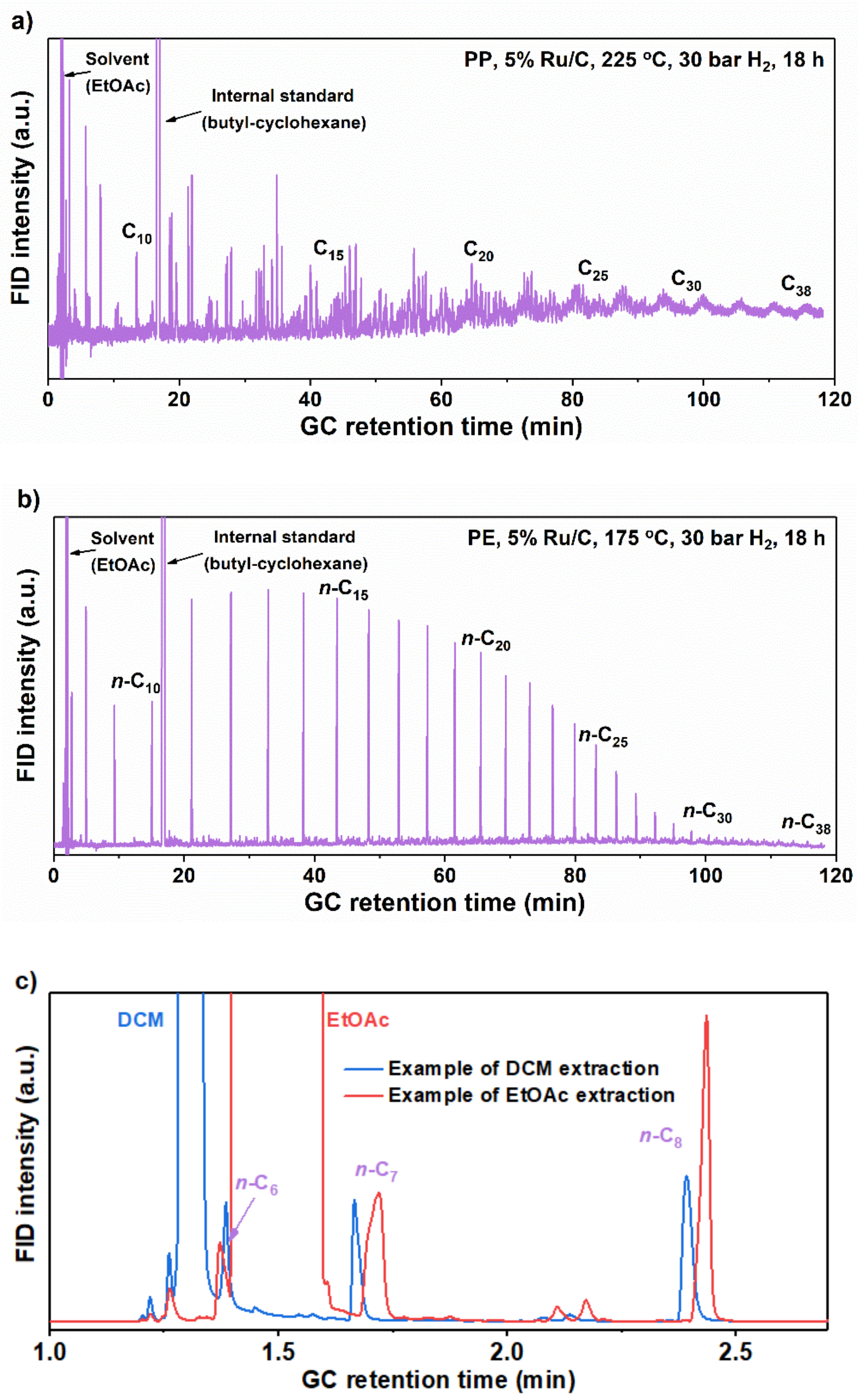

Figure S3. Examples of GC-FID chromatograms of liquid products from the hydrogenolysis of **a)** polypropylene (PP) and **b)** PE, showing the mixture of alkanes. The reaction conditions are described in each figure. Panel **c)** shows the comparison of chromatograms of samples extracted with dichloromethane (DCM, blue) and ethyl acetate (EtOAc, red).

Table S2. GC retention time and response factors of the FID detector of each *n*-alkane

C number	GC retention time (min)	FID RSF	R^2
7	2.8	0.846 [a]	0.997
8	5.0	0.905 [a]	0.997
9	9.3	0.459 [a]	0.996
10	15.0	0.508 [a]	0.994
11	21.2	0.681	0.997
12	27.2	0.678	0.997
13	32.9	0.674	0.996
14	38.3	0.668	0.996
15	43.4	0.658	0.997
16	48.3	0.651	0.973
17	52.9	0.644	0.997
18	57.3	0.632	0.997
19	61.5	0.628	0.997
20	65.5	0.627	0.997
21	69.3	0.617	0.995
22	73.0	0.615	0.997
23	76.5	0.61	0.997
24	79.9	0.608	0.997
25	83.2	0.602	0.996
26	86.3	0.601	0.997
27	89.3	0.595	0.997
28	92.3	0.602	0.997
29	95.1	0.605	0.996
30	97.8	0.609 [b]	0.997

[a] The significantly different response factors of C_7–C_{10} from other alkanes is likely caused by the GC heating ramp.

[b] For $>C_{30}$ alkanes, GC retention time was determined with a low-concentration standard, and the RSF is assumed to be identical with C_{30}, as the RSF does not change significantly with carbon number after C_{23}.

Representative gas chromatograph-flame ionization detection (GC-FID) chromatograms, covering C_{10} products from PP and PE, are shown in Figures S3a and S3b, respectively, with major products listed in Table S3 (the complementary discussion details the product identification and categorization). C_{10} products were chosen for this analysis because their boiling points is relatively high avoiding significant evaporation during handling and storage. Also, their structures are simple, and the number of possible products is small enough, for accurate identification with GC-MS.

The structure of major C_{10} products were identified by gas chromatography-mass spectroscopy (GC-MS). For PP, the dominant C_{10} product is formed only by C−C cleavage: 2,4,6-trimethylheptane (1 in Table S3), the PP fragment with 3.5 units, no side $-CH_3$ loss or isomerization. Three less concentrated but still major products also are formed by only C−C cleavage: 2,4-dimethyloctane, 3,5-dimethyloctane, and 2,6-dimethyloctane (2−4), which are all PP fragments with 4 units, the loss of one side $-CH_3$ group, but no isomerization. Theoretically, non-isomerized products should also include PP fragments with 4.5 units and the loss of two side $-CH_3$ groups (i.e., methyl-nonanes). Nevertheless, the concentration of these compounds is below the FID detection limit, but the more sensitive GC-MS shows weak corresponding peaks. Because all other C_{10} products require isomerization to form, the combined fraction of 1−4 in all C_{10} products is used as a proxy to gauge the extent to which isomerization occurs. The highest-intensity peak besides 1−4, at 10.3 min, is probably from 2,2-dimethyloctane. We note that the two peaks between 13.2 and 13.7 min are not from C_{10}—they are from the two main C_{11} products with 4 PP units, no loss of side $-CH_3$ groups or isomerization.

For PE, the dominant C_{10} product is *n*-decane, which does not require isomerization to form. Branched C_{10} alkanes from isomerization can be grouped into three categories: 1) linear C_{10} with one side chain (11.5 to 13.5 min retention time in Figure S3b), linear C_{10} with two side chains (9.7 to 11.4 min), and C_{10} cyclohexanes with more than one side chains(13.7 to 15.3 min). The retention time of the three groups is consistent with the rules of alkane boiling point with the branching structure. We note that linear C_{10} with three side chains (e.g., 1, should have lower boiling point, and thus shorter retention time, than *n*-nonane). Nonetheless, GC-MS shows that all peaks in that range are C_9. Also, C_{10} cyclohexanes with one side chain should have longer retention time than *n*-decane, but all peaks in that range are branched C_{11}. Therefore, these two types of C_{10} are absent in the products. The fraction of each group of C_{10} is used as a proxy to gauge the product branching level.

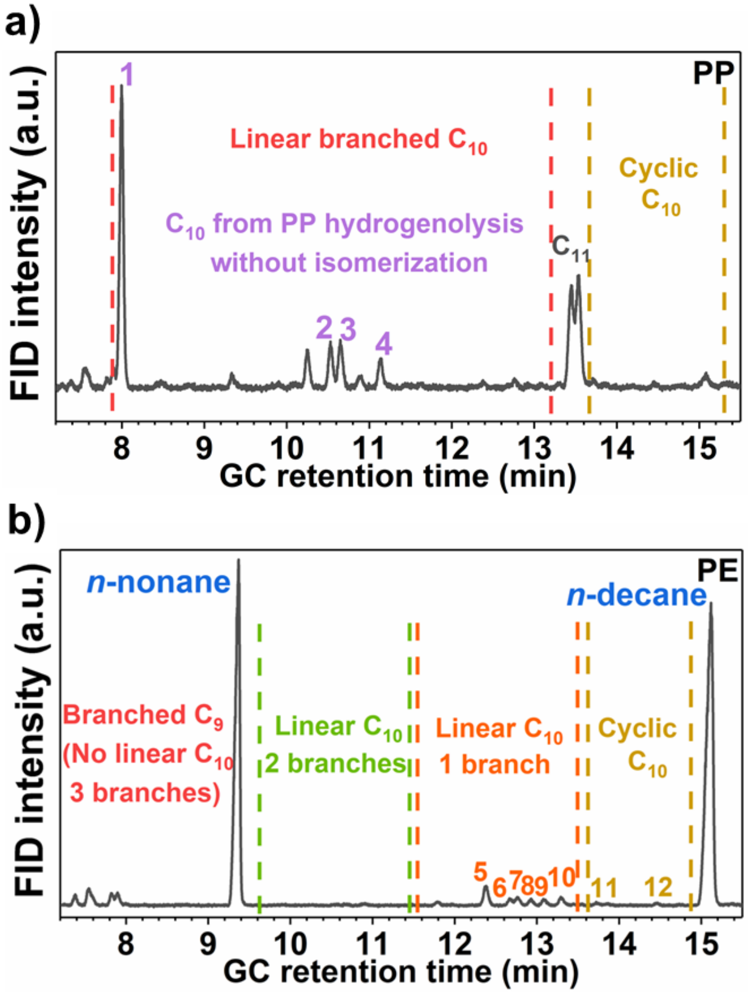

Figure S4. Representative GC-FID chromatograms in the C_{10} range of products from **a)** PP and **b)** PE hydrogenolysis. Reaction conditions: 225°C for PP and 175°C for PE, 30 bar H_2, 18 h, 1 g polyolefin, 100 mg 5 wt.% Ru/C. For PP, purple: non-isomerized alkanes (i.e., 1–4 in Table S3; red: isomerized alkanes). For PE, blue: *n*-decane; yellow: branched C_{10} cyclohexanes; orange: linear C_{10} alkanes with one branch; green: linear C_{10} alkanes with two branches. No linear C_{10} alkanes with more than two branches were identified. The identity of each C_{10} product can be found in Table S3.

Table S3. Identity and structure of major C_{10} products besides *n*-decane

	# in Figure S4	**Name**	**Structure**
PP	**1**	2,4,6-trimethylheptane	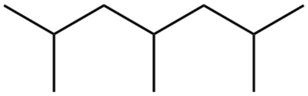
	2	2,4-dimethyloctane	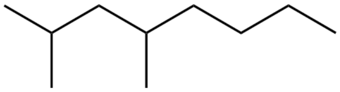
	3	3,5-dimethyloctane	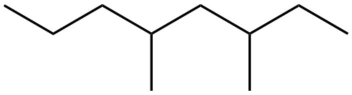
	4	2,6-dimethyloctane	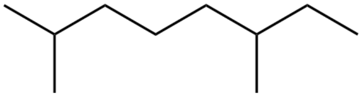 2
PE	**5**	4-ethyloctane	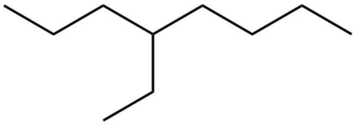
	6	5-methylnonane	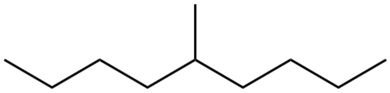
	7	4-methylnonane	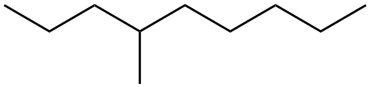
	8	2-methylnonane	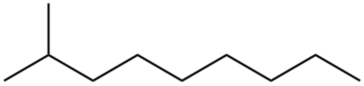
	9	3-ethyloctane	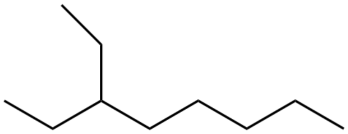
	10	3-methylnonane	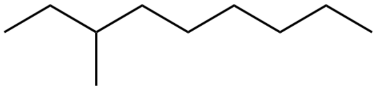
	11	1,3,6-trimethylcyclohexane	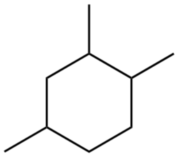
	12	1-isobutyl-3-methylcyclohexane	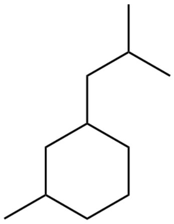

Reaction conditions: 225°C for PP and 175°C for PE, 30 bar H_2, 18 h, 1 g polyolefin, 100 mg 5 wt.% Ru/C.

Carbon yield of C_1 – C_{38} products

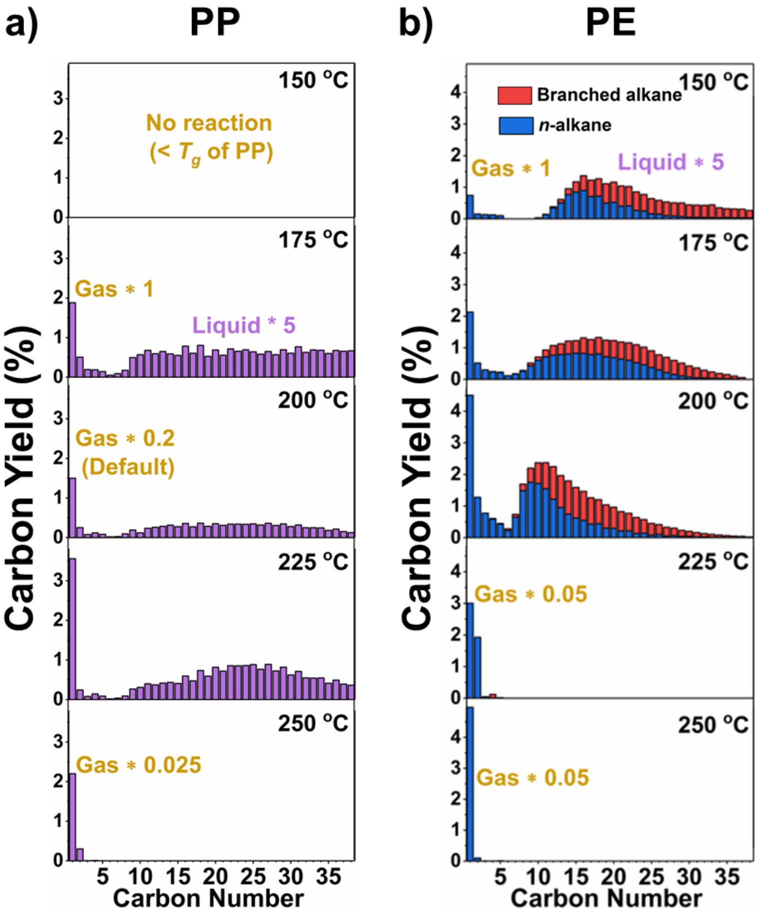

Figure S5. C yield of C_1–C_{38} products from the hydrogenolysis of **a)** PP and **b)** PE (blue: *n*-alkane; red: branched alkanes) at various temperatures. Gas products are plotted at a one-fifth scale unless noted otherwise. Reaction conditions: 30 bar H_2, 18 h, 1g PP or PE, 100 mg 5 wt.% Ru/C.

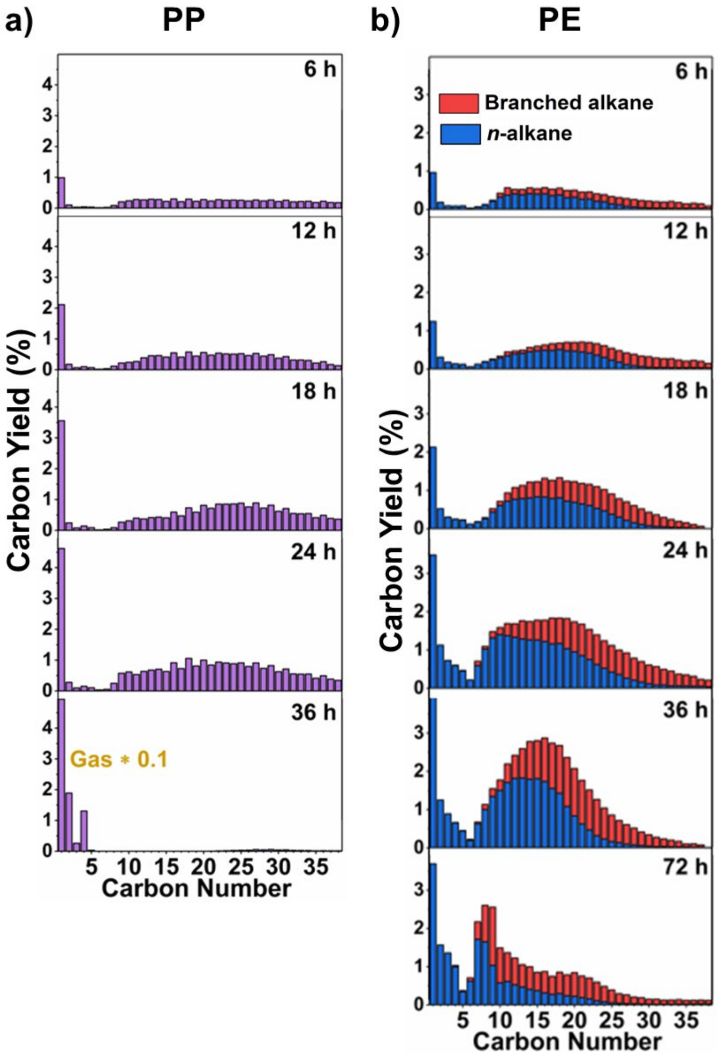

Figure S6. C yield of C_1–C_{38} products from the hydrogenolysis of **a)** PP and **b)** PE (blue: *n*-alkane; red: branched alkanes) for various time. Gas products are plotted at one-fifth scale unless noted otherwise. Reaction conditions: 225°C for PP and 175°C for PE, 30 bar H_2, 1g PP or PE, 100 mg 5 wt.% Ru/C.

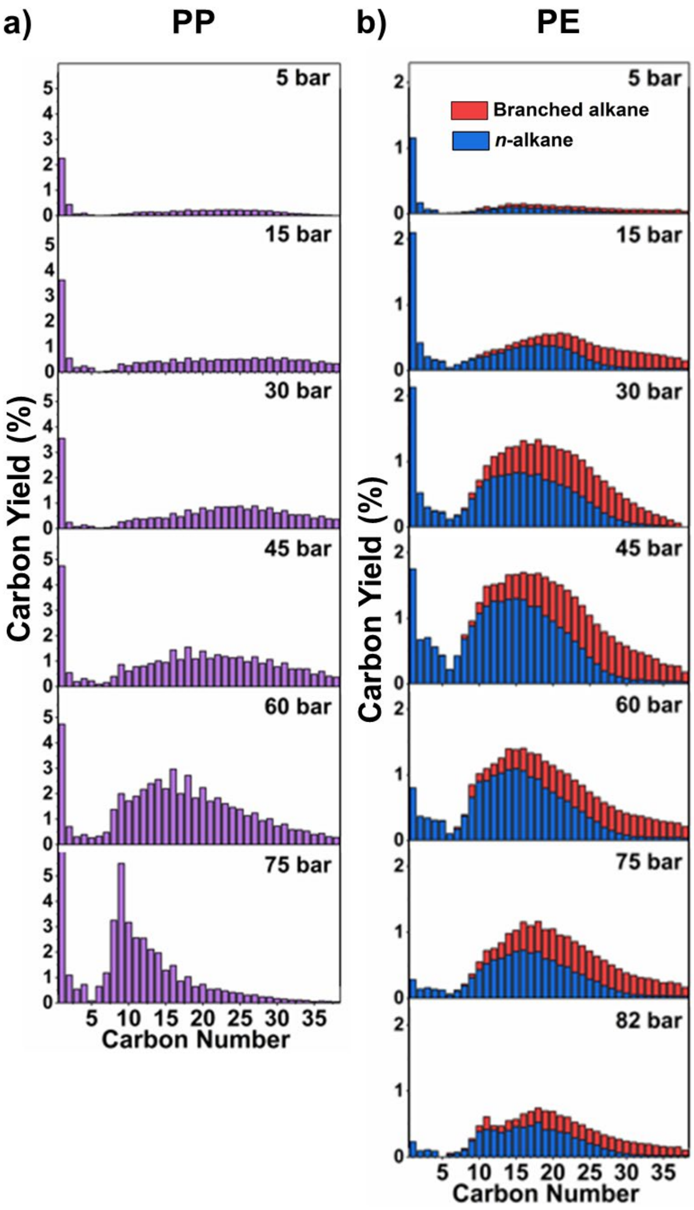

Figure S7. C yield of C_1–C_{38} products from the hydrogenolysis of **a)** PP and **b)** PE (blue: *n*-alkane; red: branched alkanes) under various H_2 pressures. Gas products are plotted at one-fifth scale unless noted otherwise. Reaction conditions: 225°C for PP and 175°C for PE, 18 h, 1g PP or PE, 100 mg 5wt.% Ru/C.

Information and discussions on the C balance

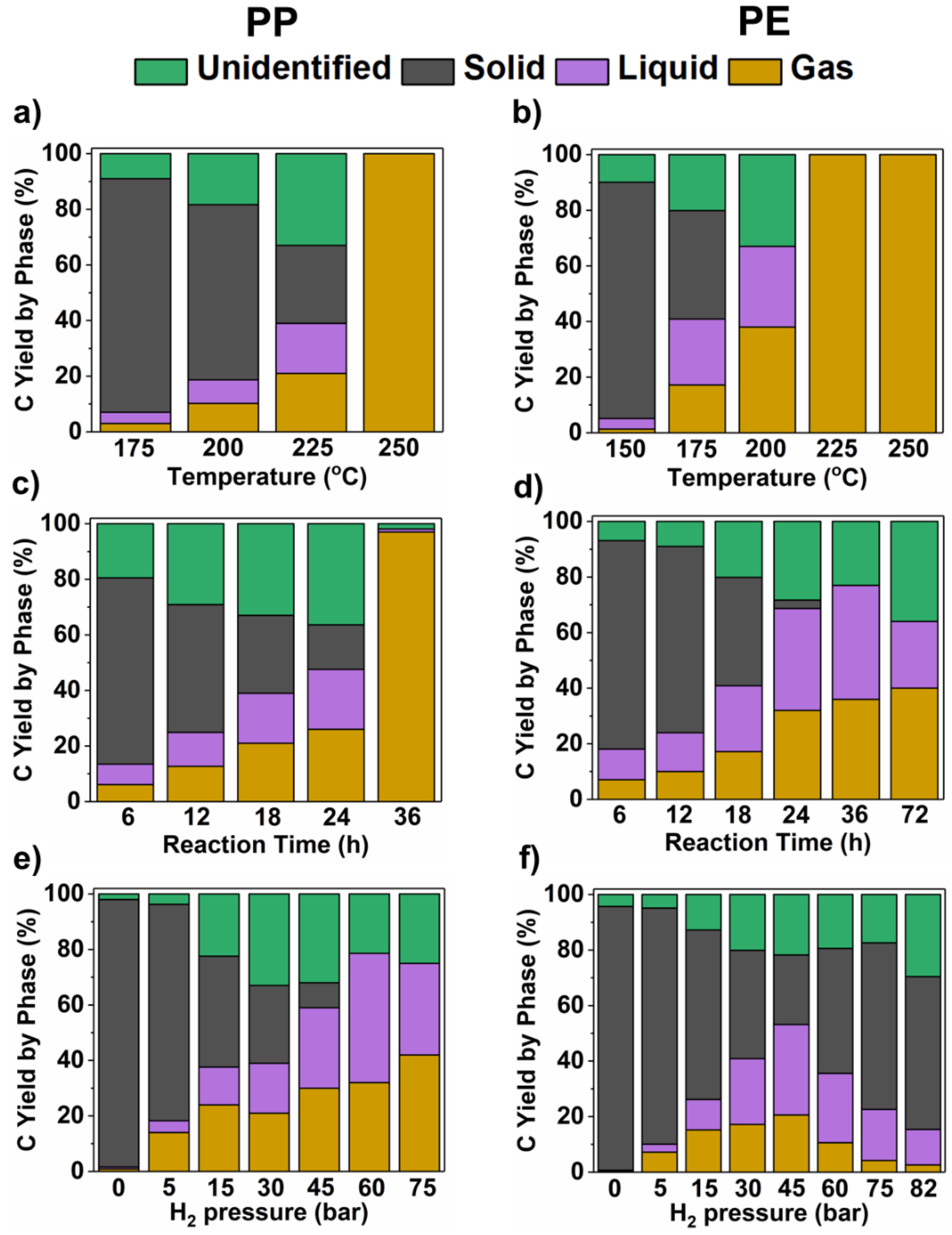

Figure S8. C yield by phase, including unidentified C for reactions in Figures 1–3 in the main text. Panel **a)** to **e)** corresponds with Figures 1a, 1b, 2a, 2b, 3a, and 3b, respectively. C balance, solid conversion, and liquid yield values are listed in Table S4.

Table S4. C balance, solid conversion, and liquid yield from all reactions in Figure S8

		PP			**PE**		
		C balance (%)	**Solid conv. (%)**	**Liquid yield (%)**	**C balance (%)**	**Solid conversion (%)**	**Liquid yield (%)**
_T_ (°C) **30 bar H_2** **18 h**	250	100.9	100	0	101.4	100	0
	225	67.0	72.5	18.4	102.1	100	0
	200	81.7	46.0	8.5	67.0	99.4	29.1
	175	91.0	15.8	4.2	79.9	61.5	23.7
	150	N/A	N/A	N/A	90.1	14.7	3.8
p_{H2} (bar) **225 °C (PP) or** **175 °C (PE)** **18 h**	0	98.0	3.6	0.7	95.7	5.6	0.4
	5	96.3	22.7	4.3	95.1	14.6	2.9
	15	77.6	60.0	13.6	87.2	39.8	11.2
	45	68.1	91.5	28.9	78.2	75.1	32.6
	60	78.6	100	46.6	80.6	55.6	25.3
	75	75.1	100	33.1	82.6	40.0	18.4
	80	N/A	N/A	N/A	70.4	36.5	12.8
_T_ (h) **225 °C (PP) or** **175 °C (PE)** **30 bar H_2**	6	80.5	34.4	7.4	93.1	25.9	11.1
	12	70.9	54.6	12.2	91.0	32.5	13.9
	24	63.6	84.1	21.6	71.7	96.6	36.7
	36	98.1	100	1.1	77.0	100	41.0
	72	N/A	N/A	N/A	64.1	100	24.2

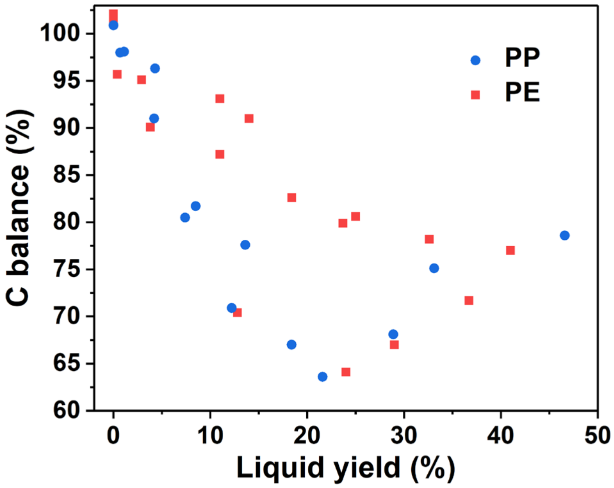

Figure S9. Negative correlation between C balance and liquid yield from the hydrogenolysis of PP and PE.

Not all products were quantified by our analysis. We think that the unidentified compounds are mostly liquid products because Figure S9 shows that reactions with higher liquid yield generally have lower C balances, while reactions that mostly produce solid and gas all have >90% C balances in Table S4. Therefore, the actual liquid selectivity/yield should be higher than values shown in the figures in the manuscript if all products can be quantified with no loss. The following factors are contributors to the loss of liquid C: 1) C_6 to C_9 alkanes are volatile and partially evaporate during handling; 2) GC peaks of several branched C_7 alkanes may be covered by the EtOAc peak. These two factors mean that $<C_{10}$ alkanes are underestimated in the C distribution. Also, alkanes that are soluble in EtOAc but $>C_{38}$ cannot be quantified by our GC. Finally, the loss of liquid products is unavoidable due to significant sticking to the walls of reactor and container.

Results of hydrogenolysis of polyethylene and polypropylene with polyvinyl chloride (PVC) addition

Table S5. Results of the hydrogenolysis of PP and PE with PVC addition

Main feedstock	PVC wt.%	Carbon yield (%)			CH_4 Selectivity (%)	Branched fraction in liquids (%)	Non-isomerized fraction in C_{10} (%)	Cyclic fraction in C_{10} (%)
		Solid	Liquid	Gas				
PP	0	27.6	17.9	20.1	46	N/A	69	12
	0.1	87.7	3.9	7.3	43	N/A	38	30
	1	96.7	1.9	0.7	7	N/A	16	45
	HCl [a]	99.0	1.7	0	0	N/A	20	58
PE	0	39.0	23.7	17.2	26	45	81	4.5
	0.1	67.6	12.3	4.6	17	44	83	7.4
	0.5	90.5	3.3	1.0	20	64	40	37
	1	93.2	2.3	0.6	18	65	56	24
	HCl [a]	95.2	1.5	0.5	18	58	15	44

[a] 0.16 g 1 M hydrochloric acid (HCl) solution containing the equal amount of Cl with 1 wt.% PVC added

Reaction conditions: 225°C and 175°C for PP and PE respectively, 30 bar H_2, total 1 g of PP/PE + PVC mixed with 100 mg Ru/C

The PVC used in the tests was purchased from Sigma Aldrich (M_W ~48,000). After these reactions, or after heating PVC by itself without any catalysts or PP/PE to 175°C, HCl "smoke" was obviously observed and strong HCl odor was noted when opening the autoclave, indicating the decomposition of PVC at beyond 175°C. The results in Table S5 clearly shows the negative effects of PVC on the hydrogenolysis activity of Ru/C. At 0.1 PVC wt.%, the effect is significant. At 1 PVC wt.% for PP and 0.5 wt.% for PE, Ru/C loses most hydrogenolysis activity. Adding 1 M HCl with Cl content equal to 1 wt.% PVC also leads to the loss of activity, confirming that the effect is from Cl instead of C produced by PVC decomposition. Meanwhile, with the presence of PVC, the CH_4 selectivity decreases, and more isomerized products, especially cyclic alkanes, are produced.

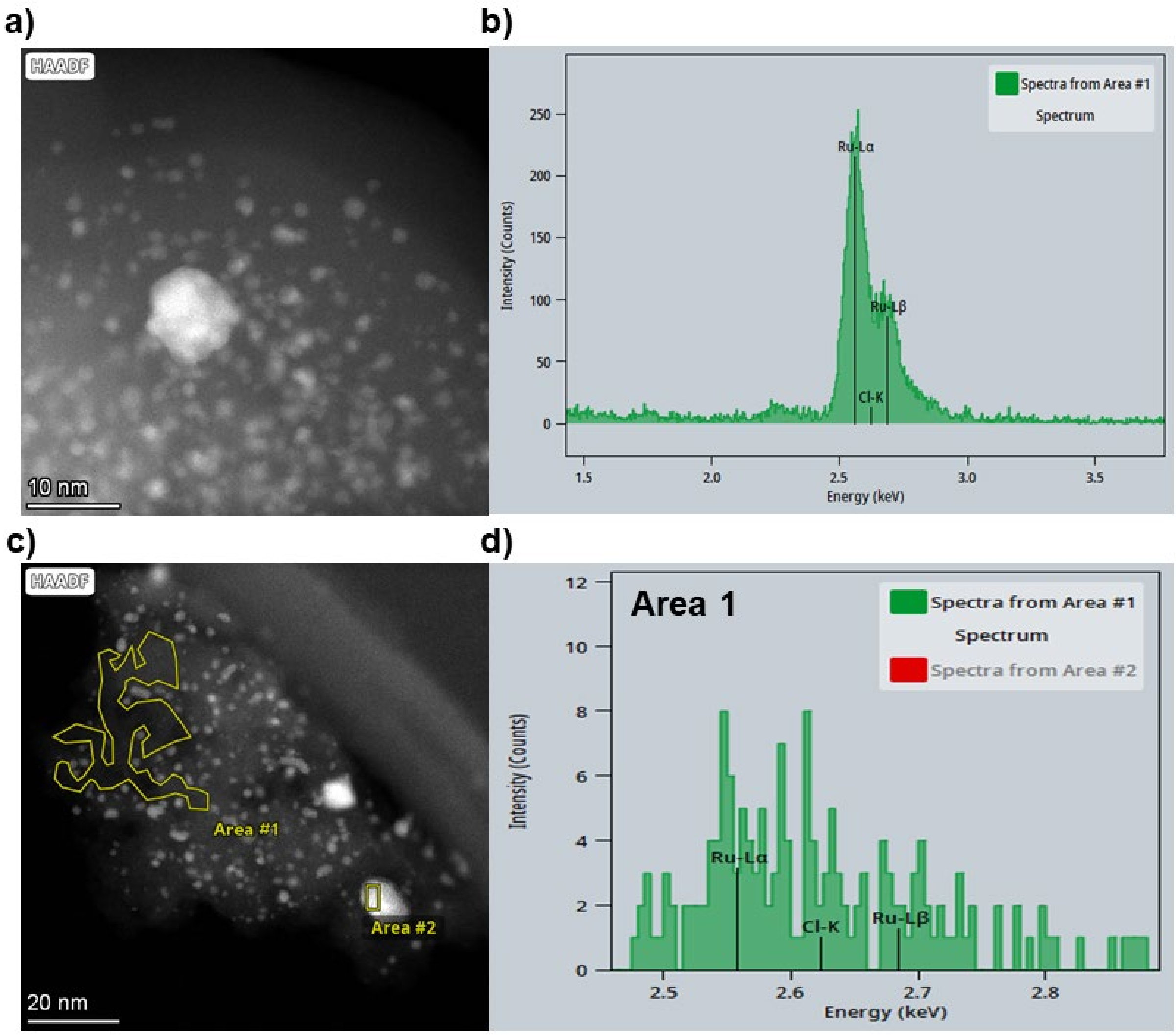

Figure S10. Scanning transmission electron microscopy/electron dispersive X-ray (EDX) measurements of a Ru/C catalyst spent in a reaction with PVC addition. Panels a) and b) show the image and the EDX map of an entire region with a large amount of Ru. Panel d) shows the EDX map of an area in panel c) that is free of Ru particles in the high-angle annular dark field microscopy image.